RESEARCH ARTICLE

Winds induce CO₂ exchange with the atmosphere and vadose zone transport in a karstic ecosystem

Enrique P. Sánchez-Cañete[1,2], Cecilio Oyonarte[3], Penélope Serrano-Ortiz[4,5], Jorge Curiel Yuste[6], Oscar Pérez-Priego[7], Francisco Domingo[8], and Andrew S. Kowalski[2,5]

[1]B2 Earth Science, Biosphere 2, University of Arizona, Tucson, Arizona, USA, [2]Departamento de Física Aplicada, Universidad de Granada, Granada, Spain, [3]Departamento Agronomía, Universidad de Almería, Almería, Spain, [4]Departamento de Ecología Terrestre, Universidad de Granada, Granada, Spain, [5]Centro Andaluz de Medio Ambiente (IISTA-CEAMA), Granada, Spain, [6]Museo Nacional de Ciencias Naturales (MNCN), CSIC, Madrid, Spain, [7]Max Planck Institute for Biogeochemistry, Jena, Germany, [8]Estación Experimental de Zonas Áridas (EEZA), CSIC, Almería, Spain

Abstract Research on the subterranean CO_2 dynamics has focused individually on either surface soils or bedrock cavities, neglecting the interaction of both systems as a whole. In this regard, the vadose zone contains CO_2-enriched air (ca. 5% by volume) in the first meters, and its exchange with the atmosphere can represent from 10 to 90% of total ecosystem CO_2 emissions. Despite its importance, to date still lacking are reliable and robust databases of vadose zone CO_2 contents that would improve knowledge of seasonal-annual aboveground-belowground CO_2 balances. Here we study 2.5 years of vadose zone CO_2 dynamics in a semiarid ecosystem. The experimental design includes an integrative approach to continuously measure CO_2 in vertical and horizontal soil profiles, following gradients from surface to deep horizons and from areas of net biological CO_2 production (under plants) to areas of lowest CO_2 production (bare soil), as well as a bedrock borehole representing karst cavities and ecosystem-scale exchanges. We found that CO_2 followed similar seasonal patterns for the different layers, with the maximum seasonal values of CO_2 delayed with depth (deeper more delayed). However, the behavior of CO_2 transport differed markedly among layers. Advective transport driven by wind induced CO_2 emission both in surface soil and bedrock, but with negligible effect on subsurface soil, which appears to act as a buffer impeding rapid CO_2 exchanges. Our study provides the first evidence of enrichment of CO_2 under plant, hypothesizing that CO_2-rich air could come from root zone or by transport from deepest layers through cracks and fissures.

1. Introduction

Knowledge about the production and transport of CO_2 within the vadose zone remains very vague. Studies about the behavior of subterranean CO_2 generally have focused either on surface soils or on bedrock cavities, usually neglecting the interaction of both systems as a whole. The vadose zone (between the water table and the soil surface) contains highly CO_2-enriched air often with more than 5% by volume in the first tens of meters [*Ek and Gewelt*, 1985; *Denis et al.*, 2005; *Batiot-Guilhe et al.*, 2007; *Benavente et al.*, 2010]. However, until now, the relationship between the vadose zone and the atmosphere has been poorly understood because studies generally have used only the uppermost soil layers, neglecting deeper layers in the soil-atmosphere CO_2 exchanges at the ecosystem level.

Continuous monitoring of net ecosystem CO_2 exchanges with the atmosphere has been widely implemented and studied. In this regard, the eddy covariance technique is the most widely accepted method to determine net CO_2 exchanges between the biosphere and atmosphere and is applied at more than 400 experimental sites worldwide [*Baldocchi*, 2014]. High-frequency data logging has produced reliable annual carbon balances around the world, generating vast databases with special interest for modeling and upscaling studies [*Reichstein et al.*, 2005; *Schwalm et al.*, 2010; *Groenendijk et al.*, 2011; *Lasslop et al.*, 2012; *Stoy et al.*, 2013]. Besides this global monitoring network, few studies have been designed to monitor continuously the CO_2 exchanges from the soil, despite their representing an important contribution (10–90%) of total ecosystem CO_2 emissions [*Hanson et al.*, 2000; *Curiel Yuste et al.*, 2005]. Thus, despite their contribution to annual carbon balances, coherent and continuous databases of soil CO_2 effluxes still do not exist [*Gomez-Casanovas et al.*, 2013].

One reason for this is the lack of a common methodological protocol to monitor soil CO_2 dynamics, with studies thereon usually designed to understand just a particular aspect and not to address the puzzle as a

whole. For instance, studies of soil CO_2 efflux (F_{soil}) can be divided into those designed to understand either surface or subsurface soil CO_2 dynamics. Surface measurements of soil CO_2 dynamics have been made widely, focusing mainly on surface-atmosphere CO_2 exchanges, with either manual [*Davidson et al.*, 1998; *Janssens et al.*, 2001] or automated soil chamber systems [*Longdoz et al.*, 2000; *Drewitt et al.*, 2002; *Subke et al.*, 2003]. Subsurface measurements, on the other hand, have been mainly focused on understanding soil CO_2 dynamics within the first 10 cm of the soil to up to several meters depths, using manual air sampling [*Risk*, 2002; *Hirsch et al.*, 2004; *Drewitt et al.*, 2005; *Davidson et al.*, 2006] or by installation of static sensors [*Hirano et al.*, 2003; *Tang et al.*, 2003]. Manual measurements have been widely used thanks to their simplicity and versatility, despite limitations on sampling frequency (normally weekly, monthly, or seasonal) and typical bias in favor of particular environmental conditions, such as daytime and/or fair weather.

Automated systems are quickly gaining popularity due to the development of new solid-state CO_2 sensors (infrared gas analyzers (IRGAs)) of low economic and energetic costs. These sensors allow continuous CO_2 measurements, recording normally every 30 min over longer periods of time [*Daly et al.*, 2009]. The soil CO_2 efflux (F_{soil}) can then be determined using the gradient method [*Maier and Schack-Kirchner*, 2014; *Sanchez-Cañete and Kowalski*, 2014]. However, despite its widespread use, the gradient method is not yet a consolidated technique, due to uncertainties associated with the determination of the soil diffusion coefficient (D_s) based on published models. Numerous diffusion models estimate D_s from soil porosity, water content, and some texture parameter [*Penman*, 1940; *Marshall*, 1959; *Millington*, 1959; *Millington and Quirk*, 1961; *Lai et al.*, 1976; *Moldrup et al.*, 1997, 1999, 2000, 2004]. However, studies comparing different diffusion models have obtained very different results depending on the model applied [*Pingintha et al.*, 2010; *Roland et al.*, 2015], suggesting that our main weakness to determine F_{soil} is both poor understanding of how gas diffusion works in the complex soil matrix and also a lack of methodologies able to model D_s in situ for each experimental site. Despite this drawback, the gradient method has great potential to become the most used technique to monitor atmosphere-soil CO_2 exchanges within the next few years.

This technique has the potential to help us understand the sources and transport of CO_2 within the vadose zone and between soil and the atmosphere. Soil CO_2 is generally of biological origin, whether autotrophic or heterotrophic, although some studies have demonstrated that geochemical [*Roland et al.*, 2013] or geological [*Rey et al.*, 2012a] sources can be relevant. In any event, the magnitude and variability of soil CO_2 production is mainly driven by soil temperature [*Pumpanen et al.*, 2003; *Chen et al.*, 2005], soil water content [*Riveros-Iregui et al.*, 2008; *Vargas et al.*, 2012; *Leon et al.*, 2014], plant phenology [*Barron-Gafford et al.*, 2011], or soil geochemistry [*Myklebust et al.*, 2008; *Maier et al.*, 2010; *Hamerlynck et al.*, 2013; *Roland et al.*, 2013].

The gradient method can be largely used under steady state conditions; however, in some ecosystem nondiffusive soil CO_2 transport due to wind or changes in atmospheric pressure can create uncertainties in the carbon balance [*Roland et al.*, 2015]. Research on nondiffusive soil CO_2 transport has concluded that the main factors involved are wind [*Sanchez-Cañete et al.*, 2011; *Nachshon et al.*, 2012] and variations in pressure [*Takle et al.*, 2004; *Bowling and Massman*, 2011; *Sanchez-Cañete et al.*, 2013b]. Additionally, the air density may play a relevant role in convective CO_2 transport in soils with large cavities and fractures [*Weisbrod et al.*, 2009; *Sanchez-Cañete et al.*, 2013a]. All of these factors involving nondiffusive processes, along with the fact that studies generally use only the uppermost soil layers neglecting the subsurface, highlight the need to know the potential interaction between different soil layers and the atmosphere and the need to examine in a systemic and integrative way the CO_2 dynamics of the different layers within the vadose zone.

Here we study, for the first time, 2.5 years of vadose zone CO_2 dynamics (transport and emission to the atmosphere) in a karst ecosystem with a deep vadose zone and very low resistance to underground gas transport, where ventilation processes explain from 25 to 66% the annual CO_2 released by the ecosystem [*Perez-Priego et al.*, 2013]. The experimental design includes an integrative methodology to continuously measure the amount of CO_2 in vertical and horizontal soil profiles, following a CO_2 productivity gradient from plant to bare soil. Subsurface CO_2 measurements and soil CO_2 efflux campaigns allow the development of a CO_2 transfer model in situ and without soil perturbation. The results allow describing and analyzing the different processes involved in long-term CO_2 dynamics within the whole vadose zone. Specifically, this study was designed to answer two main questions: (1) How does CO_2 move through the soil matrix? and (2) Do all the different layers of the vadose zone have the same behavior?
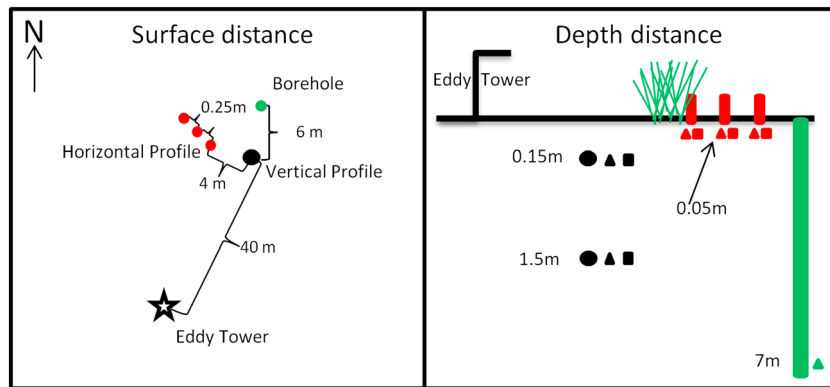
Figure 1. Schematic illustration of our experimental design. (right) The circles, triangles, and squares represent the sensors of CO_2, temperature, and soil water content, respectively.

2. Methods

2.1. Study Site

This study was conducted in *Llano de los Juanes*, a shrubland plateau at 1600 m above sea level (N36°55′41.7″, W2°45′1.7″; Sierra de Gádor, Almería, southeast Spain). The climate is subhumid with mean annual precipitation of ca. 465 mm, following the Mediterranean rainfall pattern with rain falling mostly during autumn and winter, and with a hot and dry summer with occasional thunderstorms at the end of the summer. Snow falls during winter, frequently persisting some days and covering the ground completely. The mean annual temperature is around 12°C with maximum in summer (31°C) and minimum in winter (−6°C). Following the Köppen-Geiger climate classification this site has warm temperate climate with dry and warm summers [Csb, *Kottek et al.*, 2006]. The vegetation, with a mean height of 0.5 m, is distributed in patches and is dominated by small grasses and shrubs like *Festuca scariosa* (18.8%), *Hormathophilla spinosa* (6.8%), and *Genista pumila* (5.5%). The parent soil material consists of Triassic carbonate rocks in a karstic plateau. The soil varies from 15 to 150 cm depth; the dominant soil typologies are a complex of Lithic Haploxerolls and Typic Argixerolls with inclusions of Calcic Argixerolls, where the bare soil, gravel, and rock cover 49.1% of the surface. The highest aquifers in Sierra de Gador are situated at 900 m above sea level; therefore, the vadose zone thickness or the depth to groundwater table in our experimental site exceeds 700 m. More detailed site information can be found in the work of *Serrano-Ortiz et al.* [2009]. A schematic illustration of the installations described in the following three subsections is shown in Figure 1.

2.2. Ecosystem CO_2 Fluxes

An eddy covariance system was installed in May of 2004, mounted on a top of a 2.5 m micrometeorology tower. Densities of CO_2 and water vapor as well as barometric pressure were measured by an open-path infrared gas analyzer (IRGA Li-Cor 7500; Lincoln, NE, USA). Wind speed and sonic temperature were measured by a three-axis sonic anemometer (CSAT-3; Campbell Scientific, Logan, UT, USA; hereafter CSI). The friction velocity (u_*) was determined as the turbulent velocity scale resulting from square root of the (density-normalized) momentum flux magnitude [*Stull*, 1988]. Temperature and relative humidity were measured by a thermohygrometer (HMP45C, CSI). At 1.5 m above ground level two quantum sensors (LI-190, Li-Cor), a net radiometer (NR-Lite, Kipp & Zonnen, Netherlands), and a tipping-bucket rain gauge (ARG100, CSI), measuring incident and reflected photon flux densities, net radiation, and rain, respectively, were also installed. Finally, two soil heat flux plates at 8 cm (HFP01, CSI), an averaging soil thermocouple probe (TCAV, CSI), and three water content reflectometers (CS616, CSI) were installed belowground. A data logger (CR3000, CSI) managed the eddy covariance measurements and recorded data at 10 Hz. Environmental and soil measurements were made every 10 s and recorded as 30 min averages. The ecosystem has hundreds of meters of homogeneous surface upwind of the tower in every direction. A footprint model verified that fluxes originated within from the fetch, even during periods of atmospheric stability. The flux source area model [*Schmid*, 1994] estimated the maximum source location as 27 m near end and the maximum source location far end as 114 m of 90% contributing area ellipse, during moderate turbulence ($0.2 \, \text{m s}^{-1} < u_* < 0.4 \, \text{m s}^{-1}$) for downward sensible heat fluxes ($H < 0$). Quality control of the eddy flux data was performed according to *Serrano-Ortiz et al.* [2009].

2.3. Soil CO_2 in the Whole Vadose Zone

2.3.1. Vertical CO_2 Profile in Depth

Forty meters northwest of the eddy tower, instrumentation was installed to measure subterranean CO_2 and complementary variables. A hole was bored into outcropping bedrock with 7 m depth and a diameter of 0.1 m. Solid rock cores were extracted with only a few small fractures filled by clay infiltration. The upper 1 m was hermetically isolated from the atmosphere with a metal tube cemented to the walls of the borehole and a protective cap screwed onto the tube. The CO_2 molar fraction (GMT-221; Vaisala, Inc., Finland; hereafter Vaisala) and the air temperature (107 temperature probe, CSI) were monitored inside the borehole. At 6 m to the southwest of the borehole, a vertical profile was established in the soil at depths of 0.15 m and 1.5 m. Each depth was instrumented with a CO_2 sensor (GMP-343, Vaisala), thermistor (107, CSI), and water content reflectometer (CS616, CSI). Also, a barometer was installed at the surface level (PTB101B, Vaisala). Measurements were made every 30 s and stored as 5 min averages by a data logger (CR23X, CSI).

2.3.2. Horizontal CO_2 Transect in Shallowest Layer

At 4 m to the northwest of the vertical profile, a horizontal surface transect was established from the plant to bare soil. Along the transect, CO_2 sensors (GMM-222, Vaisala), thermistors (107, CSI), and water content reflectometers (CS616, CSI) were installed at 5 cm depth, at three points: under the plant (*F. scariosa*) and at 25 and 50 cm separated from the plant. To avoid problems with the water, the CO_2 sensors were installed vertically with an in-soil adapter (211921GM, Vaisala). All the measurements were made every 30 s and stored as 5 min averages by a data logger (CR1000, CSI). Also, a soil collar to measure soil CO_2 effluxes was installed near each CO_2 sensor.

2.4. Soil CO_2 Efflux Determination From the Horizontal CO_2 Transect in the Shallowest Layer

Soil CO_2 effluxes were calculated following *Sanchez-Cañete and Kowalski* [2014]:

$$F = -D_s \cdot \rho_a \frac{d\chi_C}{dz} \quad (1)$$

where F is the upward gas flux ($\mu mol\ m^{-2}\ s^{-1}$), D_s is the soil CO_2 diffusion coefficient ($m^2\ s^{-1}$), ρ_a is the mean air molar density ($mol\ m^{-3}$), and $d\chi_C/dz$ is the vertical CO_2 molar fraction gradient ($ppm\ m^{-1}$). The CO_2 gradient was calculated using the difference between the mean atmospheric CO_2 molar fraction and the value of each soil CO_2 sensor at 5 cm depth. Vaisala sensors were configured to obtain the CO_2 molar fraction at 25° C and 101.3 kPa and later corrected for variations in temperature and pressure. Vaisala accuracy is ±1.5% of the range (0–10,000 ppm) plus ±2% of the reading. At the end of our experiment a calibration at 500 $\mu mol\ CO_2\ mol^{-1}$ showed ±3.8% of the reading (error <19 ppm). The atmospheric CO_2 molar fraction was obtained from the eddy covariance IRGA, calibrated monthly using an N_2 standard for zero and (variable but known) ~500 $\mu mol\ CO_2\ mol^{-1}$ gas standard for span. The air density (ρ_a) was obtained from the ideal gas law, and the empirical soil CO_2 transfer coefficient (k_s), which is equal to the soil CO_2 diffusion coefficient (D_s) in absence of production/consumption processes in the monitored layer, was obtained from the flux-gradient relationship proposed by *Roland et al.* [2015]:

$$k_s = -\frac{Fdz}{\rho_a d\chi_c} \quad (2)$$

wherein our study F was measured by a portable soil CO_2 flux chamber (EGM-4; PP-systems, Hitchin, UK) during six campaigns with differing soil water content. This transfer coefficient (k_s) depends not only on diffusion but also can vary with production/consumption processes in the layer, in our case from 0 to 5 cm. This equation is correct in situations of limited depth interval but is not recommended over larger depths [*Solomon and Cerling*, 1987; *Cerling*, 1991]. In every campaign, each soil collar was measured twice (located next to each CO_2 sensor in the horizontal transect; $n = 6$). The chamber system was configured to store temperature, relative humidity, CO_2, and pressure every 3 s during 120 s. The chamber fluxes were estimated as

$$F_{ch} = \frac{d\chi_c'}{d_t} \cdot \frac{V}{S} \cdot \frac{P_0(1-w_0)}{RT_0} \quad (3)$$

where F_{ch} is the soil CO_2 efflux ($\mu mol\ m^{-2}\ s^{-1}$) derived from the chamber system, $d\chi_c'/d_t$ is the initial rate of change in CO_2 molar fraction referenced to dry air ($\mu mol\ mol^{-1}\ s^{-1}$), V is the total volume (chamber + collar, m^3), S is the projected surface area (m^2), P_0 is the initial atmospheric pressure (Pa), w_0 is the initial water vapor

mole fraction (mol mol^{-1}), R is the universal gas constant (8.314, m^3 Pa K^{-1} mol^{-1}), and T_0 is the initial air temperature (K). Therefore, knowing F_{ch} and applying equation (2), we obtain the soil CO_2 transfer coefficient (K_s).

The relative gas diffusion coefficient (D_s/D_a) defines the tortuosity, where D_a is the diffusion coefficient of CO_2 in free air, calculated following Jones [1992]. The empirical relative gas transfer coefficient (k_s/D_a) was fit using a power function against soil air porosity (ε).

$$\frac{k_s}{D_a} = a \cdot \varepsilon^b \tag{4}$$

where ε is obtained as the soil porosity (Φ, cm^3 cm^{-3}) minus the soil water content (θ, cm^3 cm^{-3}) and the coefficients a and b were obtained by least squares regression. Finally, we used our calculated soil CO_2 transfer coefficient (k_s) to estimate soil CO_2 fluxes during whole the period isolating F from equation (2).

2.5. Physical-Chemical Soil Parameters

Soil samples were collected both in vertical profile and horizontal transects. Soil samples were taken for each morphological horizon in the vertical profile and under plant and bare soil in the horizontal transect. Each soil sample was obtained by composing four cores extracted with a cylindrical metal sampler. This sampler was used to obtain soil sample composites and determine bulk densities. Porosity was estimated through volumetric measurements of core samples, considering that the particle density of mineral soil is limestone with a typical value of 2.7 (g cm^{-3}). Particle-size determination was made through the pipette method after the removal of organic matter with H_2O_2 and dispersion by sodium hexametaphosphate (NaPO$_3$)$_6$. Soil sample composites were passed through a 2 mm sieve and analyzed for carbonate content (Co$_3^{-2}$) and total nitrogen (N) following *Klute* [1986] through an organic elemental analyzer (Thermo Scientific) [*Flash*, 2000]. The soil organic carbon was determined according to the modified Walkley-Black method with a correction factor of 1.3 [*Mingorance et al.*, 2007].

2.6. Statistical Analysis

The whole database was stratified, discerning between "*windy days*," days with $u^* > 0.5$ m s^{-1}, and "*before windy days*," days prior to the *windy day* and with $u^* < 0.3$ m s^{-1}. To avoid changes in soil CO_2 molar fraction due to rain, days with variation in the soil water content between *before windy day* and *windy day* exceeding 0.005 m^3 m^{-3} were excluded. Statistical tests on the effects of the wind on soil CO_2 molar fraction and net ecosystem carbon balance (NECB) were performed using pair-sample t tests for equal means, and when the data were nonnormally distributed, the nonparametric pair-sample Wilcoxon signed rank test was used. Data analysis was processed using OriginPro 2015 (OriginLab Corp., Northampton, Massachusetts, USA) and MATLAB R2015a (MathWorks, Natick, Massachusetts, USA).

3. Results

3.1. Annual Patterns of CO_2 in the Whole Vadose Zone

Annual patterns of temperature, water content, and soil CO_2 molar fraction at different soil depths are shown in Figure 2. With a slight lag, the temperature patterns of the borehole and the soil at 1.5 m were very similar, with maxima around 20℃ and minima of 7℃. The soil temperature at 0.15 m showed greater variation with maxima of 28℃ and minima of 1℃. The soil water content reached its maximum from December to April (0.5 m^3 m^{-3}) and its minimum at the end of September (0.19 m^3 m^{-3}). The soil CO_2 molar fractions (χ_c) at all depths showed a clear annual pattern with a lag in their maxima with depth, with 1500 ppm at 0.15 m, 22,000 ppm at 1.5 m, and 22,000 ppm in the borehole, occurring in June, July, and August, respectively. At 1.5 m, χ_c reached its annual peak immediately before the decrease in soil water content (SWC) and started to descend coinciding with the decrease in SWC at the same depth. In the borehole, several episodes of rapid decreases in χ_c, losing more than 10,000 ppm in a few days, were measured every year from August to October.

3.2. Annual Patterns of CO_2 Efflux From the Surface Soil to the Atmosphere

The empirical transfer model (k_s) obtained for our experimental site is shown in Figure 3. All the diffusion models fell into the 95% confidence interval of our model with low values of soil air porosity; however, two of them [*Penman*, 1940; *Moldrup et al.*, 2000] departed from the 95% confidence interval with high values
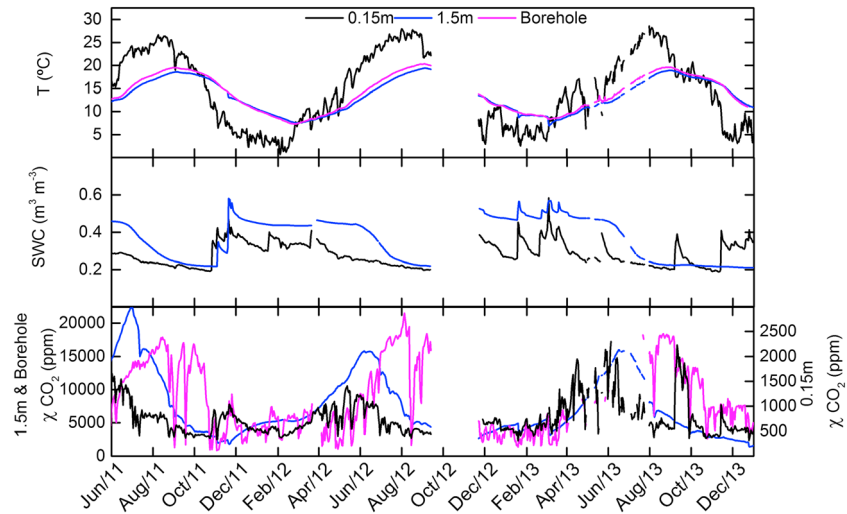
Figure 2. Daily-averaged values of temperature (T), soil water content (SWC), and CO_2 molar fraction (χ_c) in the vertical profiles of 0.15 m, 1.5 m, and 7 m (borehole) depth.

of soil air porosity (dry soil). Our empirical transfer model (Gador) showed a good fit ($R^2 = 0.96$ and RMSE $= 0.025$) with soil air porosity ($\varepsilon = \Phi - \theta$) ranging from 0.57 in dry conditions (SWC $= 0.05 \, \mathrm{m^3 \, m^{-3}}$) to 0.39 in wet conditions (SWC $= 0.23 \, \mathrm{m^3 \, m^{-3}}$). Porosity values are shown in Table 1. The k_s model obtained can be written as

$$k_s = D_a 1.658 (\Phi - \theta)^{2.087} \tag{5}$$

and through equation (2), soil CO_2 effluxes were calculated across the horizontal transect.

Regardless of proximity to a plant, soil CO_2 effluxes showed an annual pattern with maxima around $3 \, \mu\mathrm{mol} \, CO_2 \, \mathrm{m^{-2} \, s^{-1}}$ in June–July, coinciding with the beginning of the dry season (constant decrease in SWC) and high values of temperature (Figure 4). Minimum values were close to $0.25 \, \mu\mathrm{mol} \, CO_2 \, \mathrm{m^{-2} \, s^{-1}}$ and occurred from December to March, coinciding with the cold and rainy season (Figure 4). However, immedi-
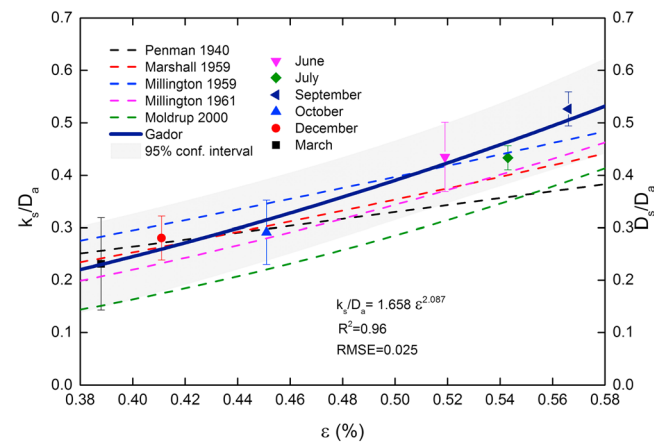

Figure 3. Values of empirical relative gas transfer coefficient (k_s/D_a), empirical transfer model obtained for our experimental site (continuous blue line), its 95% confidence interval (blue shadow), and values of relative gas diffusion coefficient (D_s/D_a) for five diffusion models commonly used (dashed lines) at different soil air porosity (ε). Mean and standard error are shown for the relative gas transfer coefficient (k_s/D_o) in six campaigns during 2012 and one on March 2013. Each campaign is the result of six measurements of the soil CO_2 efflux. The coefficients a and b shown in equation (4) were 1.658 and 2.087, respectively.

ately after the first rains after the dry season (September–October), the soil CO_2 efflux in all locations increased quickly, the most relevant event occurring in September 2013. Finally, notice that numerous peaks of the soil CO_2 efflux under plant, not associated with increases in the SWC, were measured from June to September every year. At 30 min scale, time series of soil CO_2 efflux showed diurnal differences with maximums during some hours after noon and minimums during nighttime (Figure 5). High soil CO_2 effluxes found under plant (mainly in red color) coincided with low soil CO_2 effluxes both near plant and in bare soil.

3.3. The Role of Wind in the Whole Vadose Zone and Its Relevance for the NECB

For the period where soil CO_2 effluxes reached their maximum values

Table 1. Physical Characteristics of Soil Samples Extracted Previously to the Sensor Installation[a]

	Horizon	Profile (cm)	OC (%)	C/N	Texture (%)			$CO_3^=$ (%)	BD	Porosity
					Clay	Silt	Sand			
Vertical profile	Ah[b]	0–15	3.88	11.8	52.3	38.5	9.2	1.6	1.02	0.62
	Bt	15–48	0.34	5.7	31.2	32.6	36.2	0.5	1.35	0.50
	Btg2	48–135	0.26	4.3	35.3	31.3	33.4	0.5	1.30	0.52
	2BC[b]	130–155	0.54	10.8	27.5	33.3	39.2	18.3	1.35	0.50
Horizontal transect	BC_Ah[c]	0–5	4.9	15.5	52.0	37.9	10.1	0.7	1.02	0.62
	WC_Ah[d]	0–5	3.2	11.2	48.0	41.8	10.2	0.7	1.01	0.63

[a]Organic carbon (OC), relation of carbon/nitrogen (C/N), carbonates ($CO_3^=$), and bulk density (BD).
[b]Sensor locations.
[c]Under plant sensor.
[d]Bare soil sensors.

(June–July), the amount of soil CO_2 efflux near plants was clearly determined by the wind speed and provoked net emission of CO_2 to the atmosphere measured by the eddy tower (Figure 6). The eddy covariance tower registered net CO_2 emissions to the atmosphere (positive values in the net ecosystem carbon balance (NECB)) during windy days like 7, 20, and 30 June and 5, 9, and 14 July (Figure 6a). These windy days showed the same pattern for the soil CO_2 efflux under plant (Figure 6b), whereas for the other locations, both the CO_2 efflux (Figure 6b) and the CO_2 molar fraction (Figure 6c) were inversely correlated with the W_s. When the wind speed increased it induced decreases in the CO_2 molar fraction at 0.15 m, in the borehole, and in the CO_2 efflux near plant and in bare soil (7 and 30 of June and 5, 9, and 14 of July). At 1.5 m the variations in the CO_2 molar fraction induced by the wind were produced, but they were small and not appreciable at the scale of Figure 6. During the period shown, the only days that registered rains were on 18 and 20 June with 2 and 3.5 mm, respectively. These rains provoked increments in the CO_2 effluxes independent of location and an increment in the CO_2 molar fraction at 0.15 m.
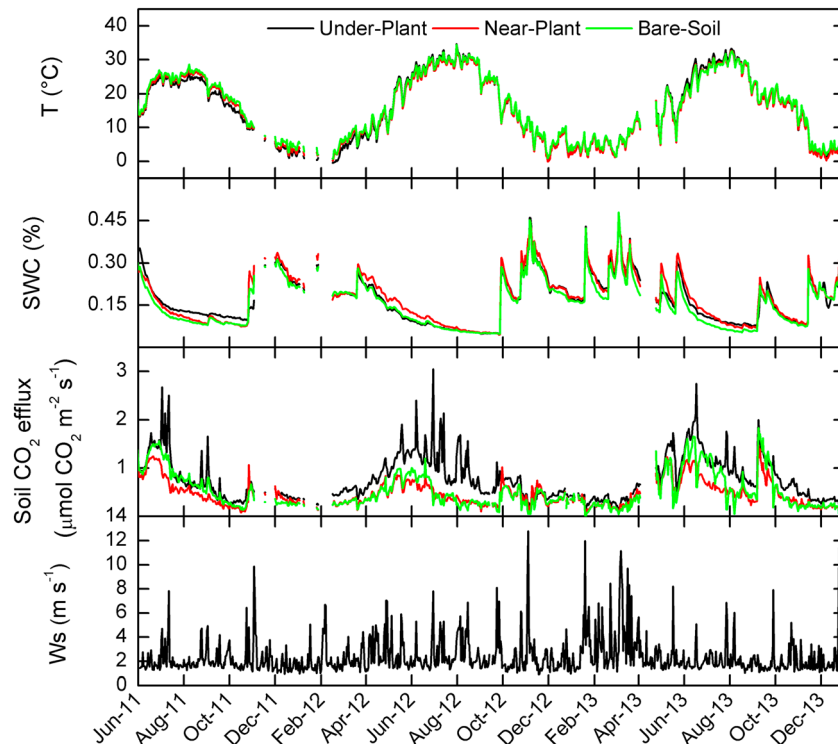

Figure 4. Daily-averaged values of temperature (T), soil water content (SWC), and soil CO_2 efflux ($\mu mol\ CO_2\ m^{-2}\ s^{-1}$) in the horizontal profile at 0.05 m depth and wind speed (W_s).
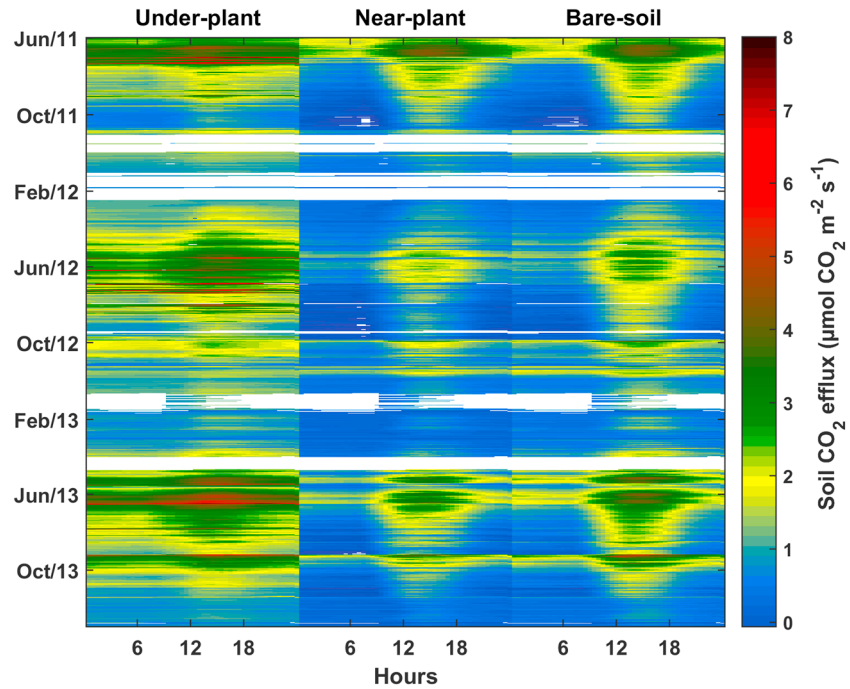
Figure 5. Time series of half-hour values of soil CO_2 efflux in the horizontal profile at 0.05 m depth from 1 June 2011 to 31 December 2013.
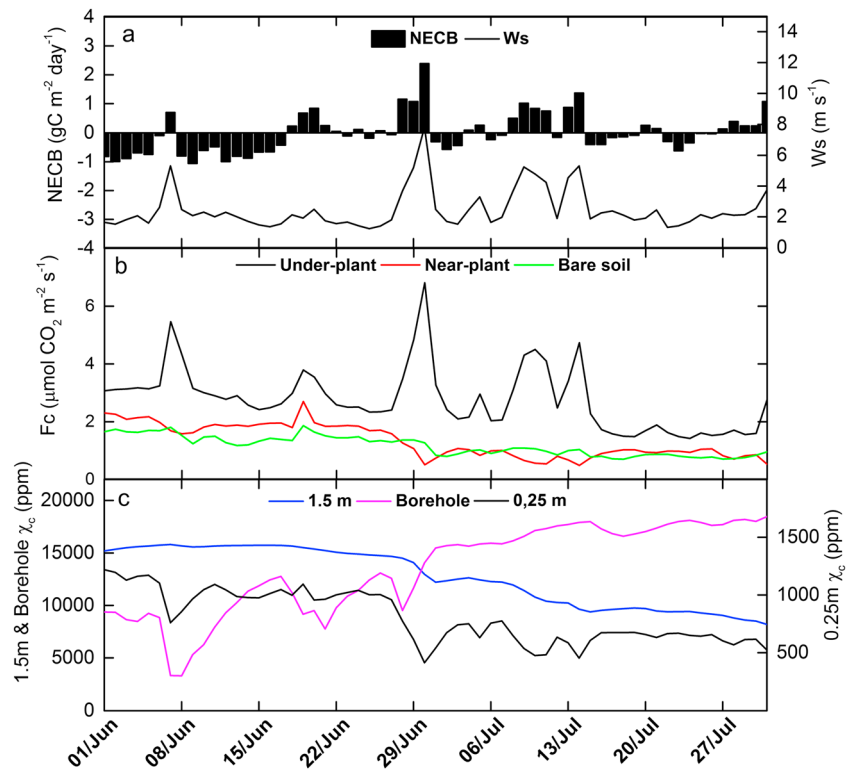

Figure 6. Daily-averaged values of net ecosystem carbon balance (NECB) and wind speed (W_s), both measured by eddy covariance, soil CO_2 efflux (F_c) in the horizontal profile, and CO_2 molar fraction (χ_c) in the vertical profile during two dry months in 2012.
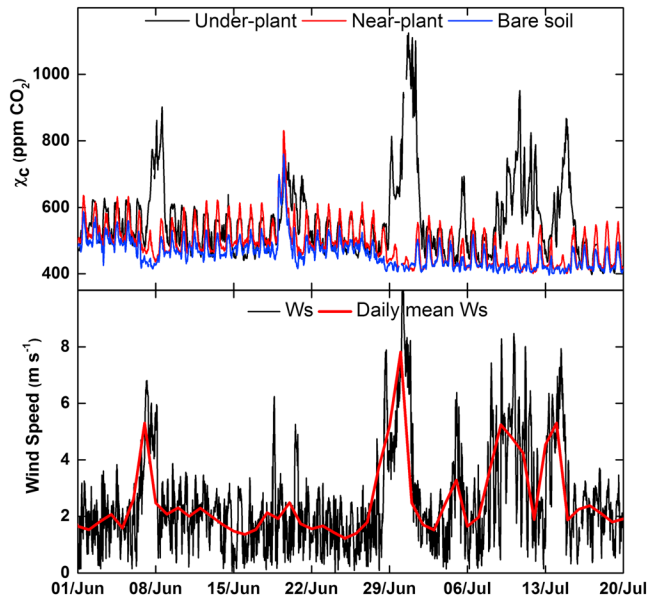
Figure 7. Half-hour average values of soil CO_2 molar fraction (χ_c) in the horizontal profile and wind speed (W_s) during 50 days in 2012.

The effect of the wind speed on the CO_2 molar fraction under plant was clearly appreciated at half hourly time scale (Figure 7). High wind speeds induced abrupt increases in the soil CO_2 molar fraction under plant, whereas for the other locations (near plant and bare soil), a slight decrease was observed (Figure 7). During windy days (6–8 June, 28 June, 3 July, and 8–15 July), the CO_2 under plant can easily double its previous mean values, wiping out the clear daily pattern of the previous days. However, near the plant and in bare soil, windy days provoked decreases in the daily maxima of soil CO_2 molar fractions while maintaining the daily patterns. The increments in the CO_2 molar fraction measured by all sensors in horizontal profile during the days 18–20 June were due to rain.

To verify that during windy days the soil CO_2 molar fraction decreases and this soil CO_2 is emitted to the atmosphere resulting in higher CO_2 emission fluxes at ecosystem level with respect to previous calm days, we compared windy days with days prior to these windy days (Figure 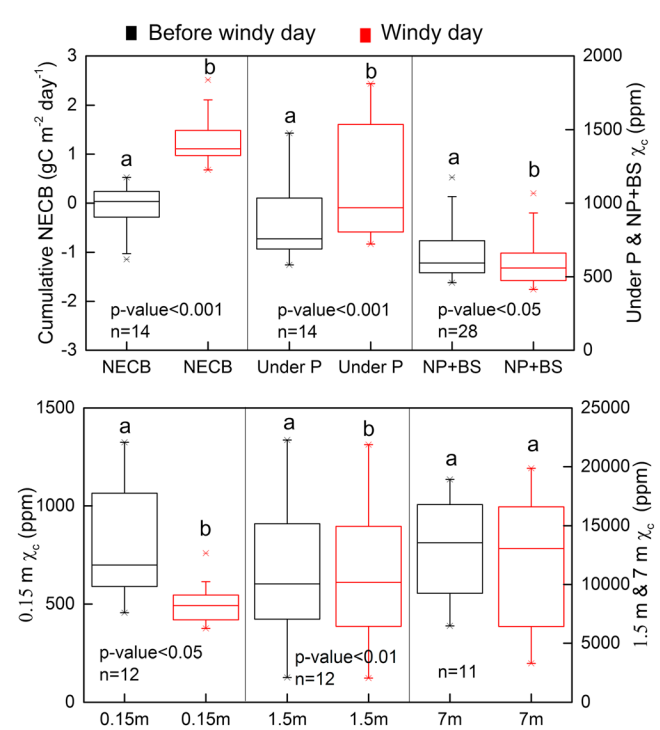8). Significant differences were found in the plot-scale soil CO_2 molar fraction and the ecosystem-scale NECB. Windy days produced significant increases both in the NECB and in the CO_2 molar fraction registered by the sensor located under plant. However, windy days produced decreases in the soil CO_2 molar fraction in all the other location: 0.15 m, 1.5 m, and 7 m and at shallow depth in bare soil (0.05 m, considering bare soil as the sum of near plant and bare soil).

Figure 8. Box plot of daily mean of cumulative NECB and soil CO_2 molar fraction (χ_c) at different locations: under plant (under P), considering bare soil as the sum of near plant (NP), and bare soil (BS) at 0.15 m, 1.5 m, and 7 m. The middle line of box plot indicates the median; the upper and lower box bounds are the 25th and 75th percentiles. The error bars mark the 5th and 95th percentiles of the distributions, with 1st and 99th percentiles indicated by cross.

4. Discussion

4.1. How Does CO_2 Move Through the Soil Matrix?

Our results showed that soil CO_2 dynamics were not always exclusively due to diffusion. Advection should be taken into account when winds or gradients in pressure or temperature exceeds certain limits, inducing releases of significant amounts of CO_2 and affecting both surface soil horizons and the subsurface of the vadose zone. Recent research on soil CO_2 dynamics within the soil matrix, using different techniques, has similarly concluded

that the main factors involved in nondiffusive transport were wind, pressure, and temperature. Wind has been correlated with changes in soil CO_2 molar fraction in forest [*Subke et al.*, 2003; *Jassal et al.*, 2005; *Goffin et al.*, 2014], meadow [*Roland et al.*, 2015], volcanoes [*Risk et al.*, 2013], snow-covered sites [*Seok et al.*, 2009; *Bowling and Massman*, 2011], and drylands [*Sanchez-Cañete et al.*, 2011; *Rey et al.*, 2012b]. Similarly, correlations between atmospheric pressure and the soil CO_2 mole fraction have been observed in wetlands [*Comas et al.*, 2011], forests [*Maier et al.*, 2010], volcanoes [*Rogie et al.*, 2001], snow-covered sites [*Massman et al.*, 1997; *Fujiyoshi et al.*, 2010], and semiarid ecosystems [*Sanchez-Cañete et al.*, 2013b]. In parallel, advective/convective transport of CO_2 due to air temperature has been documented in large cavities [*Kowalski and Sanchez-Cañete*, 2010; *Sanchez-Cañete et al.*, 2013a], soil fractures [*Weisbrod et al.*, 2009; *Moore et al.*, 2011], and laboratories [*Ganot et al.*, 2014]. Therefore, all of these authors highlight the importance of nondiffusive transport in exchanges between the soil and atmosphere.

4.2. Do All the Different Layers of the Vadose Zone Have the Same Behavior?

The different layers forming the vadose zone—surface soil, subsurface soil, and bedrock—showed similar seasonal patterns of CO_2, where maximum values were delayed with depth (the deeper, the more delayed in time). In terms of CO_2 transport patterns (Figure 2), however, the dynamics differed among soil layers. For the shallowest sensor at 0.15 m, the maximum values of CO_2 molar fraction during the year preceded the maximum values of soil temperature and were obtained under relatively low SWC values. This period (June) coincided with the end of the growing season [*Serrano-Ortiz et al.*, 2009], when vegetation begins its senescence due to the depletion of soil water reserves [*Canton et al.*, 2010]. Deeper soil CO_2 molar fractions at 1.5 m followed seasonal patterns similar to that of the shallow layer, preceding the temperature seasonal maximum at its same depth. Molar fractions of CO_2 also decreased with SWC, when the pore space filled by air increases and facilitates diffusion to the atmosphere [*Kowalski et al.*, 2008; *Maier et al.*, 2010; *Cuezva et al.*, 2011]. On the contrary, in the borehole seasonal variations of CO_2 molar fraction strongly covaried with borehole temperature, reaching their maximum values during the same period of the year.

The seasonal covariation between CO_2 molar fraction and temperature for the borehole, in contrast with the seasonal decoupling between those two variables in the two different soil layers (0.15 m and 1.5 m), indicated that the mechanisms of CO_2 production and processes driving CO_2 dynamics differed markedly between depths. On one hand, the decrease in CO_2 molar fractions in both soil layers coinciding with the decrease in SWC suggests that CO_2 dynamics in those two layers of the vadose zone were directly related to biological CO_2 production. This behavior is supported by the well-known strong relation between soil CO_2 production from autotrophic (plants) and heterotrophic (microbes) biological sources with water availability [*Curiel Yuste et al.*, 2007] in water-limited ecosystems. On the other hand, the covariation of CO_2 molar fraction with temperature in the borehole reflects a common behavior of karst caves, where accumulation and ventilation are mainly determined by differences in the temperature between the internal and external atmosphere [*Serrano-Ortiz et al.*, 2010b]. When the air temperature decreases during winter, cold air from the exterior descends into the borehole displacing the warmer borehole air which rises and exits; however, during summer the cold air remains in the borehole avoiding the exchange with the atmosphere. Therefore, at the seasonal scale, the annual cycle of CO_2 in the borehole seems to be decoupled from biological sources and is determined by the accumulation of air enriched in CO_2 during summer and subsequent ventilation due to convective transport during winter.

Although the large variations in the borehole CO_2 molar fraction were decoupled from biological sources, the stable isotope composition of CO_2 ($\delta^{13}CO_2$) at this site showed a biological origin of air coming from both bedrock and surface soil [*Serrano-Ortiz et al.*, 2010a]. These data suggest that the great amounts of CO_2 in deep layers are of biological origin. Therefore, we hypothesize that CO_2 produced by roots in the surface soil must percolate down through unsaturated soil layers due to the added density associated with CO_2 enrichment [*Kowalski and Sanchez-Cañete*, 2010; *Sanchez-Cañete et al.*, 2013a]. For this reason, more CO_2 is always found in deeper layers around the world whether in soil [*Atkinson*, 1977] or caves [*Ek and Gewelt*, 1985]. Therefore, the high CO_2 concentration found both in the soil at 1.5 m and in the borehole of this karstic site (Figure 2) seem to come via percolation from overlying layers due to its biological origin, despite CO_2 emissions to the atmosphere, resulting in the CO_2 accumulation in the soil. However, we cannot yet rule out the possibility that the biological origin of CO_2 at depth be attributed to living beings at depth, which can be
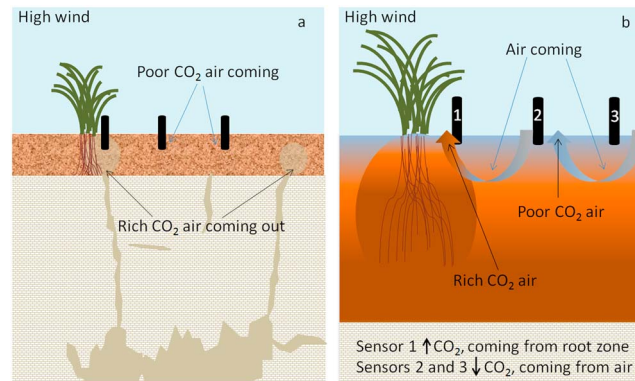
Figure 9. Hypotheses to explain soil CO_2 increases only under plant and induced by wind. (a) Sensor located on top of a fissure. (b) The CO_2 is transported from root zone. High CO_2 molar fractions are denoted in dark brown and low values in light blue.

found more than 1000 m below the surface [*Stoev et al.*, 2015]. To resolve this issue, future studies should focus on partitioning through manipulated pulse labeling [*Epron et al.*, 2012], since the natural abundance of carbon isotopes in the ecosystems are not a generally useful tool for partitioning between autotrophic and heterotrophic respiration [*Bowling et al.*, 2015].

At shorter time scales (days or weeks), however, advective transport induced by winds at this site provoked decreases in the soil CO_2 molar fraction at all the locations except for the sensor located under plant (Figure 8). These CO_2 losses from the soil were emitted to the atmosphere provoking an increase in emissions registered at ecosystem level. The CO_2 lost due to the wind effect was higher for both surface soils and the borehole, with a negligible effect in subsurface layers (1.5 m) due to the soil-buffering effect (Figure 6). The decrease of the CO_2 molar fraction driven by high winds occurred when the amount of CO_2 in the surface soil and the borehole reached their respective maxima (Figure 2). Thus, at 0.15 m such decreases in the CO_2 molar fraction occurred mainly from April to July, whereas for the borehole the largest events occurred from August to October (Figure 2c). The CO_2 molar fraction in the borehole can quickly decrease by more than 15000 ppm on windy days, with subsequent and fast recovery to previous values (September 2011 and 2012) probably via recharge from deeper layers (through fissures connected with the borehole), given that the lower concentrations of CO_2 from the upper soil layers with respect to the borehole preclude downward refilling. Therefore, our results showed that advective transport due to winds had a relevant role in the short-term (days-weeks) variability of soil CO_2 effluxes that should be taken into account, suggesting the need to incorporate these terms into the transport equations based on the gradient method or predictive soil CO_2 models, at least for this site.

4.3. Increments in Soil CO_2 Under Plant Driven by Wind

Our study provides the first evidence that enrichment in CO_2 from the root zone, where CO_2 is biologically produced, to the surface soil was mainly driven by wind. Increases in wind speed can double CO_2 molar fractions in the surface soil and thus, double F_{soil} exclusively under plants. In bare soils, on the other hand, windy days caused soil ventilation (CO_2 losses) and therefore a decrease in the F_{soil}, given that there is no refilling of CO_2 from biological production. The wind-induced vertical CO_2 transport in the soil reflected an increasing F_{soil} near its biological source (plant), which further affected the net ecosystem CO_2 exchange, turning ecosystems into CO_2 sources during windy periods (Figure 6). Figure 6 also illustrates the mechanisms behind the observed wind-induced ecosystem pulses of CO_2. Increases in wind speed coincided with rapid decreases in the CO_2 molar fraction with soil depth caused by soil ventilation (CO_2 loss), which was immediately detected in the sign of the net ecosystem CO_2 exchanges. The fact that only under plant did the increases in wind speed provoke increases in CO_2 molar fraction (Figures 7 and 8), and therefore in F_{soil}, further confirmed the notion that respiration was likely the main process producing CO_2.

Two main hypotheses to explain why soil CO_2 increases exclusively under plant during windy days are illustrated in Figure 9. Hypothesis A attributes the increases in CO_2 to the possible location of the sensor over a fissure, emitting CO_2-enriched air from deeper layers toward the surface; this hypothesis is drawn in Figure 9a. The location of the plant near the fissure may or may not be coincidental. Hypothesis B attributes CO_2 increases to a transport phenomenon [*Takle et al.*, 2004], where eddies can penetrate deeper into the soil due to wind blocking by the plant, increasing the pressure gradient and inducing soil aeration in deeper layers and thus transport of CO_2-enriched air of the root zone to nearby shallow areas (Figure 9b). For this reason, under high wind conditions only under the plant (sensor 1) does the CO_2 molar fraction largely

increase, while more distant sensors (bare soil, sensors 2 and 3) register decreased CO_2 molar fractions due to dilution by mixing with atmospheric air. Although these CO_2 increases are present throughout the study period, there is only one replicate under plant, and therefore, these hypotheses cannot be generalized. To test these hypotheses more investigation is required in the future. Hypothesis A could be tested with subsurface images driven by ground-penetrating radar, which could indicate the presence of fissures. Hypothesis B could be tested with a new experimental design with replicated sensors under plants and plant-sized, abiotic obstacles to the wind.

5. Conclusions

This is the first study showing evidence that the wind can cause increases in the CO_2 in the shallow soil layer. In our site, the transect from below plant to bare soil showed that during windy days, CO_2 molar fraction increased exclusively in the sensor located under the plant. We hypothesize that this could be due to CO_2 transport from the deep root zone toward the surface or maybe due to CO_2 transport from deeper layers through fissures. However, in bare soil high winds provoked decreases in the soil CO_2 molar fraction. On windy days, soil CO_2 effluxes emitted to the atmosphere from under plant were greater than on calm days, whereas emissions from bare soil were reduced. All of this highlights the importance of spatial and temporal variabilities of soil CO_2 effluxes measured with chamber systems or static CO_2 sensors and the need to adapt the scale of measurement to that of the CO_2 balance being studied. The results presented here come from a horizontal CO_2 profile of three individual points without replicates but with a long and continuous data series. For this reason, the results invite further research in this and others ecosystems regarding whether the wind causes increases in the CO_2 exclusively under plants or simply these increases in CO_2 are due to a preferential path of CO_2 emissions.

The studied karst system stored large CO_2 amounts below ground, which later were emitted to the atmosphere during windy days. During much of the year both the subsurface and bedrock CO_2 mole fractions easily exceeded 10,000 ppm, equivalent to 25 times atmospheric values (400 ppm). The soil-atmosphere CO_2 exchanges at 1.5 m were weak due to the soil-buffering effect. However, borehole-atmosphere CO_2 exchanges were produced very quickly (hourly scales), losing easily the half of the CO_2 previously stored. When winds subsided, the borehole and therefore the soil fractures were filled quickly with CO_2-enriched air stored in the deep soil. Therefore, in this karst ecosystem the soil acted as a buffer impeding the rapid CO_2 exchanges produced through fractures.

References

Atkinson, T. C. (1977), Carbon-dioxide in atmosphere of unsaturated zone—Important control of groundwater hardness in limestones, *J. Hydrol.*, *35*, 111–123, doi:10.1016/0022-1694(77)90080-4.

Baldocchi, D. (2014), Measuring fluxes of trace gases and energy between ecosystems and the atmosphere—The state and future of the eddy covariance method, *Global Change Biol.*, *20*, 3600–3609, doi:10.1111/gcb.12649.

Barron-Gafford, G. A., R. L. Scott, G. D. Jenerette, and T. E. Huxman (2011), The relative controls of temperature, soil moisture, and plant functional group on soil CO_2 efflux at diel, seasonal, and annual scales, *J. Geophys. Res.*, *116*, G01023, doi:10.1029/2010JG001442.

Batiot-Guilhe, C., J.-L. Seidel, H. Jourde, O. Hebrard, and V. Bailly-Comte (2007), Seasonal variations of CO_2 and Rn-222 in a Mediterranean sinkhole—Spring (Causse d'Aumelas, SE France), *Int. J. Speleol.*, *36*, 51–56.

Benavente, J., I. Vadillo, F. Carrasco, A. Soler, C. Linan, and F. Moral (2010), Air carbon dioxide contents in the vadose zone of a Mediterranean karst, *Vadose Zo. J.*, *9*, 126–136, doi:10.2136/vzj2009.0027.

Bowling, D. R., and W. J. Massman (2011), Persistent wind-induced enhancement of diffusive CO_2 transport in a mountain forest snowpack, *J. Geophys. Res.*, *116*, G04006, doi:10.1029/2011JG001722.

Bowling, D. R., J. E. Egan, S. J. Hall, and D. A. Risk (2015), Environmental forcing does not induce diel or synoptic variation in the carbon isotope content of forest soil respiration, *Biogeosciences*, *12*(16), 5143–5160, doi:10.5194/bg-12-5143-2015.

Canton, Y., L. Villagarcia, M. Jose Moro, P. Serrano-Ortiz, A. Were, F. Javier Alcala, A. S. Kowalski, A. Sole-Benet, R. Lazaro, and F. Domingo (2010), Temporal dynamics of soil water balance components in a karst range in southeastern Spain: Estimation of potential recharge, *Hydrol. Sci. J.-J. DES Sci. Hydrol.*, *55*(5), 737–753, doi:10.1080/02626667.2010.490530.

Cerling, T. E. (1991), Carbon dioxide in the atmosphere: Evidence from Cenozoic and Mesozoic paleosols, *Am. J. Sci. States*, *291*, 377–400.

Chen, D., J. A. E. Molina, C. E. Clapp, R. T. Venterea, and A. J. Palazzo (2005), Corn root influence on automated measurement of soil carbon dioxide concentrations, *Soil Sci.*, *170*(10), 779–787, doi:10.1097/01.ss.0000190512.41298.fc.

Comas, X., L. Slater, and A. S. Reeve (2011), Atmospheric pressure drives changes in the vertical distribution of biogenic free-phase gas in a northern peatland, *J. Geophys. Res.*, *116*, G04014, doi:10.1029/2011JG001701.

Cuezva, S., A. Fernandez-Cortes, D. Benavente, P. Serrano-Ortiz, A. S. Kowalski, and S. Sanchez-Moral (2011), Short-term CO_2(g) exchange between a shallow karstic cavity and the external atmosphere during summer: Role of the surface soil layer, *Atmos. Environ.*, *45*, 1418–1427, doi:10.1016/j.atmosenv.2010.12.023.

Curiel Yuste, J., M. Nagy, I. A. Janssens, A. Carrara, and R. Ceulemans (2005), Soil respiration in a mixed temperate forest and its contribution to total ecosystem respiration, *Tree Physiol.*, *25*, 609–619.

Curiel Yuste, J., D. D. Baldocchi, A. Gershenson, A. Goldstein, L. Misson, and S. Wong (2007), Microbial soil respiration and its dependency on carbon inputs, soil temperature and moisture, *Global Change Biol.*, *13*(9), 2018–2035, doi:10.1111/j.1365-2486.2007.01415.x.

Daly, E., S. Palmroth, P. Stoy, M. Siqueira, A. C. Oishi, J.-Y. Juang, R. Oren, A. Porporato, and G. G. Katul (2009), The effects of elevated atmospheric CO_2 and nitrogen amendments on subsurface CO_2 production and concentration dynamics in a maturing pine forest, *Biogeochemistry*, *94*(3), 271–287.

Davidson, E. A., E. Belk, and R. D. Boone (1998), Soil water content and temperature as independent or confounded factors controlling soil respiration in a temperate mixed hardwood forest, *Global Change Biol.*, *4*, 217–227, doi:10.1046/j.1365-2486.1998.00128.x.

Davidson, E. A., K. E. Savage, S. E. Trumbore, and W. Borken (2006), Vertical partitioning of CO_2 production within a temperate forest soil, *Global Change Biol.*, *12*(6), 944–956.

Denis, A., R. Lastennet, F. Huneau, and P. Malaurent (2005), Identification of functional relationships between atmospheric pressure and CO_2 in the cave of Lascaux using the concept of entropy of curves, *Geophys. Res. Lett.*, *32*, L05810, doi:10.1029/2004GL022226.

Drewitt, G. B., T. A. Black, Z. Nesic, E. R. Humphreys, E. M. Jork, R. Swanson, G. J. Ethier, T. Griffis, and K. Morgenstern (2002), Measuring forest floor CO_2 fluxes in a Douglas-fir forest, *Agr. Forest Meteorol.*, *110*, 299–317, doi:10.1016/s0168-1923(01)00294-5.

Drewitt, G. B., T. A. Black, and R. S. Jassal (2005), Using measurements of soil CO_2 efflux and concentrations to infer the depth distribution of CO_2 production in a forest soil, *Can. J. Soil Sci.*, *85*(2), 213–221.

Ek, C., and M. Gewelt (1985), Carbon-dioxide in cave atmospheres—New results in belgium and comparison with some other countries, *Earth Surf. Processes Landforms*, *10*, 173–187, doi:10.1002/esp.3290100209.

Epron, D., et al. (2012), Pulse-labelling trees to study carbon allocation dynamics: A review of methods, current knowledge and future prospects, *Tree Physiol.*, *32*(6), 776–798, doi:10.1093/treephys/tps057.

Fujiyoshi, R., Y. Haraki, T. Sumiyoshi, H. Amano, I. Kobal, and J. Vaupotic (2010), Tracing the sources of gaseous components (Rn-222, CO_2 and its carbon isotopes) in soil air under a cool-deciduous stand in Sapporo, Japan, *Environ. Geochem. Health*, *32*, 73–82, doi:10.1007/s10653-009-9266-1.

Ganot, Y., M. I. Dragila, and N. Weisbrod (2014), Impact of thermal convection on CO_2 flux across the Earth-atmosphere boundary in high-permeability soils, *Agr. Forest Meteorol.*, *184*, 12–24, doi:10.1016/j.agrformet.2013.09.001.

Goffin, S., M. Aubinet, M. Maier, C. Plain, H. Schack-Kirchner, and B. Longdoz (2014), Characterization of the soil CO_2 production and its carbon isotope composition in forest soil layers using the flux-gradient approach, *Agr. Forest Meteorol.*, *188*, 45–57, doi:10.1016/j.agrformet.2013.11.005.

Gomez-Casanovas, N., K. Anderson-Teixeira, M. Zeri, C. J. Bernacchi, and E. H. DeLucia (2013), Gap filling strategies and error in estimating annual soil respiration, *Global Change Biol.*, *19*, 1941–1952, doi:10.1111/gcb.12127.

Groenendijk, M., et al. (2011), Assessing parameter variability in a photosynthesis model within and between plant functional types using global FluxNet eddy covariance data, *Agr. Forest Meteorol.*, *151*, 22–38, doi:10.1016/j.agrformet.2010.08.013.

Hamerlynck, E. P., R. L. Scott, E. P. Sanchez-Cañete, and G. A. Barron-Gafford (2013), Nocturnal soil CO_2 uptake and its relationship to subsurface soil and ecosystem carbon fluxes in a Chihuahuan desert shrubland, *J. Geophys. Res. Biogeosciences*, *118*, 1593–1603, doi:10.1002/2013jg002495.

Hanson, P. J., N. T. Edwards, C. T. Garten, and J. A. Andrews (2000), Separating root and soil microbial contributions to soil respiration: A review of methods and observations, *Biogeochemistry*, *48*(1), 115–146, doi:10.1023/A:1006244819642.

Hirano, T., H. Kim, and Y. Tanaka (2003), Long-term half-hourly measurement of soil CO_2 concentration and soil respiration in a temperate deciduous forest, *J. Geophys. Res.*, *108*(D20), 4631, doi:10.1029/2003JD003766.

Hirsch, A. I., S. E. Trumbore, and M. L. Goulden (2004), The surface CO_2 gradient and pore-space storage flux in a high-porosity litter layer, *Tellus, Ser. B*, *56*, 312–321, doi:10.1111/j.1600-0889.2004.00113.x.

Janssens, I. A., A. S. Kowalski, and R. Ceulemans (2001), Forest floor CO_2 fluxes estimated by eddy covariance and chamber-based model, *Agr. Forest Meteorol.*, *106*, 61–69, doi:10.1016/s0168-1923(00)00177-5.

Jassal, R., A. Black, M. Novak, K. Morgenstern, Z. Nesic, and D. Gaumont-Guay (2005), Relationship between soil CO_2 concentrations and forest-floor CO_2 effluxes, *Agr. Forest Meteorol.*, *130*, 176–192, doi:10.1016/j.agrformet.2005.03.005.

Jones, H. G. (1992), *Plants and Microclimate: A Quantitative Approach to Environmental Plant Physiology*, 2nd ed., Cambridge Univ. Press, New York.

Kottek, M., J. Grieser, C. Beck, B. Rudolf, and F. Rubel (2006), World map of the Köppen-Geiger climate classification updated, *Meteorol. Z.*, *15*, 259–263, doi:10.1127/0941-2948/2006/0130.

Kowalski, A. S., and E. P. Sanchez-Cañete (2010), A new definition of the virtual temperature, valid for the atmosphere and the CO_2-rich air of the vadose zone, *J. Appl. Meteorol. Climatol.*, *49*, 1692–1695, doi:10.1175/2010jamc2534.1.

Kowalski, A. S., P. Serrano-Ortiz, I. A. Janssens, S. Sanchez-Moral, S. Cuezva, F. Domingo, A. Were, and L. Alados-Arboledas (2008), Can flux tower research neglect geochemical CO_2 exchange?, *Agr. Forest Meteorol.*, *148*, 1045–1054, doi:10.1016/j.agrformet.2008.02.004.

Lai, S.-H., J. M. Tiedje, and A. E. Erickson (1976), In situ measurement of gas diffusion coefficient in soils, *Soil Sci. Soc. Am. J.*, *40*, 3–6, doi:10.2136/sssaj1976.03615995004000010006x.

Lasslop, G., et al. (2012), On the choice of the driving temperature for eddy-covariance carbon dioxide flux partitioning, *Biogeosciences*, *9*, 5243–5259, doi:10.5194/bg-9-5243-2012.

Leon, E., R. Vargas, S. Bullock, E. Lopez, A. R. Panosso, and N. La Scala Jr. (2014), Hot spots, hot moments, and spatio-temporal controls on soil CO_2 efflux in a water-limited ecosystem, *Soil Biol. Biochem.*, *77*, 12–21, doi:10.1016/j.soilbio.2014.05.029.

Longdoz, B., M. Yernaux, and M. Aubinet (2000), Soil CO_2 efflux measurements in a mixed forest: Impact of chamber disturbances, spatial variability and seasonal evolution, *Global Change Biol.*, *6*(8), 907–917, doi:10.1046/j.1365-2486.2000.00369.x.

Maier, M., and H. Schack-Kirchner (2014), Using the gradient method to determine soil gas flux: A review, *Agr. Forest Meteorol.*, *192*, 78–95, doi:10.1016/j.agrformet.2014.03.006.

Maier, M., H. Schack-Kirchner, E. E. Hildebrand, and J. Holst (2010), Pore-space CO_2 dynamics in a deep, well-aerated soil, *Eur. J. Soil Sci.*, *61*, 877–887, doi:10.1111/j.1365-2389.2010.01287.x.

Marshall, T. J. (1959), The diffusion of gases through porous media, *J. Soil Sci.*, *10*(1), 79–82, doi:10.1111/j.1365-2389.1959.tb00667.x.

Massman, W. J., R. A. Sommerfeld, A. R. Mosier, K. F. Zeller, T. J. Hehn, and S. G. Rochelle (1997), A model investigation of turbulence-driven pressure-pumping effects on the rate of diffusion of CO_2, N_2O, and CH_4 through layered snowpacks, *J. Geophys. Res.*, *102*, 18,851–18,863, doi:10.1029/97JD00844.

Millington, R. J. (1959), Gas diffusion in porous media, *Science*, *130*(3367), 100–102, doi:10.1126/science.130.3367.100-a.

Millington, R. J., and J. P. Quirk (1961), Permeability of porous solids, *Trans. Faraday Soc.*, *57*, 1200–1207, doi:10.1039/tf9615701200.

Mingorance, M. D., E. Barahona, and J. Fernández-Gálvez (2007), Guidelines for improving organic carbon recovery by the wet oxidation method, *Chemosphere*, *68*(3), 409–13, doi:10.1016/j.chemosphere.2007.01.021.

Moldrup, P., T. Olesen, D. E. Rolston, and T. Yamaguchi (1997), Modeling diffusion and reaction in soils.7. Predicting gas and ion diffusivity in undisturbed and sieved soils, *Soil Sci.*, *162*, 632–640, doi:10.1097/00010694-199709000-00004.

Moldrup, P., T. Olesen, T. Yamaguchi, P. Schjonning, and D. E. Rolston (1999), Modeling diffusion and reaction in soils: IX. The Buckingham-Burdine-Campbell equation for gas diffusivity in undisturbed soil, *Soil Sci.*, *164*, 542–551, doi:10.1097/00010694-199908000-00002.

Moldrup, P., T. Olesen, J. Gamst, P. Schjonning, T. Yamaguchi, and D. E. Rolston (2000), Predicting the gas diffusion coefficient in repacked soil: Water-induced linear reduction model, *Soil Sci. Soc. Am. J.*, *64*, 1588–1594.

Moldrup, P., T. Olesen, S. Yoshikawa, T. Komatsu, and D. E. Rolston (2004), Three-porosity model for predicting the gas diffusion coefficient in undisturbed soil, *Soil Sci. Soc. Am. J.*, *68*, 750–759.

Moore, J. R., V. Gischig, M. Katterbach, and S. Loew (2011), Air circulation in deep fractures and the temperature field of an alpine rock slope, *Earth Surf. Processes Landforms*, *36*, 1985–1996, doi:10.1002/esp.2217.

Myklebust, M. C., L. E. Hipps, and R. J. Ryel (2008), Comparison of eddy covariance, chamber, and gradient methods of measuring soil CO_2 efflux in an annual semi-arid grass, *Bromus tectorum*, *Agr. Forest Meteorol.*, *148*, 1894–1907, doi:10.1016/j.agrformet.2008.06.016.

Nachshon, U., M. Dragila, and N. Weisbrod (2012), From atmospheric winds to fracture ventilation: Cause and effect, *J. Geophys. Res.*, *117*, G02016, doi:10.1029/2011JG001898.

Penman, H. L. (1940), Gas and vapour movements in the soil I. The diffusion of vapours through porous solids, *J. Agric. Sci.*, *30*, 437–462.

Perez-Priego, O., P. Serrano-Ortiz, E. P. Sanchez-Cañete, F. Domingo, and A. S. Kowalski (2013), Isolating the effect of subterranean ventilation on CO_2 emissions from drylands to the atmosphere, *Agr. Forest Meteorol.*, *180*, 194–202, doi:10.1016/j.agrformet.2013.06.014.

Pingintha, N., M. Y. Leclerc, J. P. Beasley Jr., G. Zhang, and C. Senthong (2010), Assessment of the soil CO_2 gradient method for soil CO_2 efflux measurements: Comparison of six models in the calculation of the relative gas diffusion coefficient, *Tellus, Ser. B*, *62*, 47–58, doi:10.1111/j.1600-0889.2009.00445.x.

Pumpanen, J., H. Ilvesniemi, and P. Hari (2003), A process-based model for predicting soil carbon dioxide efflux and concentration, *Soil Sci. Soc. Am. J.*, *67*, 402–413.

Reichstein, M., et al. (2005), On the separation of net ecosystem exchange into assimilation and ecosystem respiration: Review and improved algorithm, *Global Change Biol.*, *11*, 1424–1439, doi:10.1111/j.1365-2486.2005.001002.x.

Rey, A., G. Etiope, L. Belelli-Marchesini, D. Papale, and R. Valentini (2012a), Geologic carbon sources may confound ecosystem carbon balance estimates: Evidence from a semiarid steppe in the southeast of Spain, *J. Geophys. Res.*, *117*, G03034, doi:10.1029/2012JG001991.

Rey, A., L. Belelli-Marchesini, A. Were, P. Serrano-Ortiz, G. Etiope, D. Papale, F. Domingo, and E. Pegoraro (2012b), Wind as a main driver of the net ecosystem carbon balance of a semiarid Mediterranean steppe in the south east of Spain, *Global Change Biol.*, *18*, 539–554, doi:10.1111/j.1365-2486.2011.02534.x.

Risk, D. (2002), Carbon dioxide in soil profiles: Production and temperature dependence, *Geophys. Res. Lett.*, *29*(6), 11-1–11-4, doi:10.1029/2001GL014002.

Risk, D., C. K. Lee, C. MacIntyre, and S. C. Cary (2013), First year-round record of Antarctic Dry Valley soil CO_2 flux, *Soil Biol. Biochem.*, *66*, 193–196, doi:10.1016/j.soilbio.2013.07.006.

Riveros-Iregui, D. A., B. L. McGlynn, H. E. Epstein, and D. L. Welsch (2008), Interpretation and evaluation of combined measurement techniques for soil CO_2 efflux: Discrete surface chambers and continuous soil CO_2 concentration probes, *J. Geophys. Res.*, *113*, G04027, doi:10.1029/2008JG000811.

Rogie, J. D., D. M. Kerrick, M. L. Sorey, G. Chiodini, and D. L. Galloway (2001), Dynamics of carbon dioxide emission at Mammoth Mountain, California, *Earth Planet. Sci. Lett.*, *188*, 535–541, doi:10.1016/s0012-821x(01)00344-2.

Roland, M., et al. (2013), Atmospheric turbulence triggers pronounced diel pattern in karst carbonate geochemistry, *Biogeosciences*, *10*, 5009–5017, doi:10.5194/bg-10-5009-2013.

Roland, M., S. Vicca, M. Bahn, T. Ladreiter-Knauss, M. Schmitt, and I. A. Janssens (2015), Importance of nondiffusive transport for soil CO_2 efflux in a temperate mountain grassland, *J. Geophys. Res. Biogeosciences*, *120*, 502–512, doi:10.1002/2014JG002788.

Sanchez-Cañete, E. P., and A. S. Kowalski (2014), Comment on "Using the gradient method to determine soil gas flux: A review" by M. Maier and H. Schack-Kirchner, *Agr. Forest Meteorol.*, *197*, 254–255, doi:10.1016/j.agrformet.2014.07.002.

Sanchez-Cañete, E. P., P. Serrano-Ortiz, A. S. Kowalski, C. Oyonarte, and F. Domingo (2011), Subterranean CO_2 ventilation and its role in the net ecosystem carbon balance of a karstic shrubland, *Geophys. Res. Lett.*, *38*, L09802, doi:10.1029/2011GL047077.

Sanchez-Cañete, E. P., P. Serrano-Ortiz, F. Domingo, and A. S. Kowalski (2013a), Cave ventilation is influenced by variations in the CO_2-dependent virtual temperature, *Int. J. Speleol.*, *42*, 1–8, doi:10.5038/1827-806x.42.1.1.

Sanchez-Cañete, E. P., A. S. Kowalski, P. Serrano-Ortiz, O. Perez-Priego, and F. Domingo (2013b), Deep CO_2 soil inhalation/exhalation induced by synoptic pressure changes and atmospheric tides in a carbonated semiarid steppe, *Biogeosciences*, *10*, 6591–6600, doi:10.5194/bg-10-6591-2013.

Schmid, H. P. (1994), Source areas for scalars and scalar fluxes, *Boundary Layer Meteorol.*, *67*, 293–318.

Schwalm, C. R., et al. (2010), Assimilation exceeds respiration sensitivity to drought: A FluxNet synthesis, *Global Change Biol.*, *16*, 657–670, doi:10.1111/j.1365-2486.2009.01991.x.

Seok, B., D. Helmig, M. W. Williams, D. Liptzin, K. Chowanski, and J. Hueber (2009), An automated system for continuous measurements of trace gas fluxes through snow: An evaluation of the gas diffusion method at a subalpine forest site, Niwot Ridge, Colorado, *Biogeochemistry*, *95*, 95–113, doi:10.1007/s10533-009-9302-3.

Serrano-Ortiz, P., F. Domingo, A. Cazorla, A. Were, S. Cuezva, L. Villagarcia, L. Alados-Arboledas, and A. S. Kowalski (2009), Interannual CO_2 exchange of a sparse Mediterranean shrubland on a carbonaceous substrate, *J. Geophys. Res.*, *114*, G04015, doi:10.1029/2009JG000983.

Serrano-Ortiz, P., S. Cuezva, A. S. Kowalski, and S. Sánchez-Moral (2010a), Cuantificación y procedencia de los intercambios de CO_2 en un ecosistema carbonatado mediante la técnica de eddy covariance y el análisis de los isótopos estables de carbono, *Ecosistemas*, *19*(3), 41–51.

Serrano-Ortiz, P., M. Roland, S. Sanchez-Moral, I. A. Janssens, F. Domingo, Y. Godderis, and A. S. Kowalski (2010b), Hidden, abiotic CO_2 flows and gaseous reservoirs in the terrestrial carbon cycle: Review and perspectives, *Agr. Forest Meteorol.*, *150*, 321–329, doi:10.1016/j.agrformet.2010.01.002.

Solomon, D. K., and T. E. Cerling (1987), The annual carbon dioxide cycle in a montane soil: Observations, modeling, and implications for weathering, *Water Resour. Res.*, *23*, 2257–2265, doi:10.1029/WR023i012p02257.

Stoev, P., N. Akkari, A. Komericki, G. Edgecombe, and L. Bonato (2015), At the end of the rope: *Geophilus hadesi* sp. n.—The world's deepest cave-dwelling centipede (Chilopoda, Geophilomorpha, Geophilidae), *Zookeys*, *510*, 95–114, doi:10.3897/zookeys.510.9614.

Stoy, P. C., et al. (2013), A data-driven analysis of energy balance closure across FluxNet research sites: The role of landscape scale heterogeneity, *Agr. Forest Meteorol.*, *171*, 137–152, doi:10.1016/j.agrformet.2012.11.004.

Stull, R. B. (1988), *An Introduction to Boundary Layer Meteorology*, Springer, Netherlands.

Subke, J. A., M. Reichstein, and J. D. Tenhunen (2003), Explaining temporal variation in soil CO_2 efflux in a mature spruce forest in southern Germany, *Soil Biol. Biochem.*, *35*, 1467–1483, doi:10.1016/s0038-0717(03)00241-4.

Takle, E. S., W. J. Massman, J. R. Brandle, R. A. Schmidt, X. H. Zhou, I. V. Litvina, R. Garcia, G. Doyle, and C. W. Rice (2004), Influence of high-frequency ambient pressure pumping on carbon dioxide efflux from soil, *Agr. Forest Meteorol.*, *124*, 193–206, doi:10.1016/j.agrformet.2004.01.014.

Tang, J. W., D. D. Baldocchi, Y. Qi, and L. K. Xu (2003), Assessing soil CO_2 efflux using continuous measurements of CO_2 profiles in soils with small solid-state sensors, *Agr. Forest Meteorol.*, *118*, 207–220, doi:10.1016/s0168-1923(03)00112-6.

Vargas, R., S. L. Collins, M. L. Thomey, J. E. Johnson, R. F. Brown, D. O. Natvig, and M. T. Friggens (2012), Precipitation variability and fire influence the temporal dynamics of soil CO_2 efflux in an arid grassland, *Global Change Biol.*, *18*, 1401–1411, doi:10.1111/j.1365-2486.2011.02628.x.

Weisbrod, N., M. I. Dragila, U. Nachshon, and M. Pillersdorf (2009), Falling through the cracks: The role of fractures in Earth-atmosphere gas exchange, *Geophys. Res. Lett.*, *36*, L02401, doi:10.1029/2008GL036096.